

**Abstract.** We present the X-ray spectrum of MR Vel/RX J0925.7–4758, obtained with the Medium Energy Grating spectrometer of the Chandra X-ray Telescope. The simplest models used by earlier authors, stellar atmospheres in combination with a thermal plasma in collisional ionization equilibrium, cannot explain the spectrum. Neither does a photo-ionized plasma. We identify P Cygni profiles of Fe XVII and O VIII, from which we conclude that these lines arise in a wind. We conclude that major uncertainty exists about the bolometric luminosity of MR Vel, and perhaps of supersoft sources in general, so that the theoretical prediction that this luminosity derives from steady nuclear burning cannot be verified.

**Key words:** stars: atmospheres — binaries: close — line: identification — stars: individual: MR Vel — stars: winds, outflows — x-rays: binaries

# The complex X-ray spectrum of the supersoft source MR Vel

Henk Bearda<sup>1</sup>, Wouter Hartmann<sup>2</sup>, Ken Ebisawa<sup>3</sup>, John Heise<sup>1,2</sup>, Jelle Kaastra<sup>2</sup>, Rob van der Meer<sup>2</sup>, Frank Verbunt<sup>1</sup>, and Christian Motch<sup>4</sup>

<sup>1</sup> Astronomical Institute, Utrecht University, P.O.Box 80000, NL-3508 TA Utrecht, The Netherlands

<sup>2</sup> SRON National Institute for Space Research, Sorbonnelaan 2, NL-CA 3584 Utrecht, The Netherlands,

<sup>3</sup> Laboratory for High Energy Astrophysics, NASA Goddard Space Flight Center, Greenbelt, MD 20771, U.S.A.

<sup>4</sup> Observatoire Astronomique, UA 1280 CNRS, 11 rue de l'Université, F-67000 Strasbourg, France

Received date October 24, 2018/ Accepted date

## 1. Introduction

Supersoft X-ray sources are called such because they emit most of their X-ray flux at energies less than 0.4 keV. First discovered with the Einstein satellite (Long et al. 1981), they were recognized as a class only after the more sensitive observations with ROSAT (Trümper et al. 1991). The suggestion that the X-ray emission of supersoft sources is caused by steady nuclear burning at the surface of white dwarfs with masses near the Chandrasekhar limit (Van den Heuvel et al. 1992, see also Shara et al. 1977, Iben 1982) gained credibility when the nova GQ Mus was found to be a supersoft source (Ögelman et al. 1993).

Van den Heuvel et al. (1992) argued that the high mass-transfer rates ( $\gtrsim 10^{-7} M_{\odot} \text{ yr}^{-1}$ ) demanded by theory for steady-state hydrogen burning require donors with masses in the range of 1.4-2.2  $M_{\odot}$ . However, optical identifications soon showed that the class of supersoft X-ray sources is far from homogeneous, in some cases exclude  $\gtrsim 1.4 M_{\odot}$  donors, and also cast doubt on the premise that the white dwarfs in these systems accrete steadily at high rates (e.g. the review by Gänsicke et al. 2000).

Black body fits indicated that the X-ray luminosities of supersoft sources – several of which are located in the Magellanic Clouds, and thus have known distances – are in excess of the Eddington limit for a white dwarf (Greiner et al. 1991). Fitting LTE white-dwarf atmosphere model spectra to the X-ray data, Heise et al. (1994) showed that the X-ray luminosities may well be at or below the Eddington limit. NLTE models may give very different luminosities again (Hartmann & Heise 1997). The rather limited spectral resolution of the Einstein and ROSAT X-ray data prevents an accurate determination of the X-ray spectrum and of the interstellar absorption, and this leads to very large uncertainty of the estimated bolometric flux. Accurate determination of the luminosities is important for comparison with the models, and to establish the re-

lation of the supersoft sources with other sources showing very soft spectra at low luminosities, such as the variable source in the globular cluster NGC 5272 whose nature is unknown (Dotani et al. 1999) or VSge whose X-rays may arise from colliding winds (e.g. Wood & Lockley 2000).

Studies of Cal87 and MR Vel/RX J0925.7–4758, both supersoft sources with significant count rates above 0.4 keV, have shown that an LTE or NLTE white-dwarf atmosphere model does not correctly describe the X-ray spectrum (Hartmann et al. 1999, Ebisawa et al. 2001). In this paper we present the first X-ray spectrum of the supersoft source MR Vel with sufficient resolution to test spectral models in some detail.

**Table 1.** Summary of models for the X-ray data of MR Vel, giving the instrument used, its wavelength range and the resolution at 1 keV, the model used and its fit parameters. BB, SA and TP indicate a black body, NLTE stellar atmosphere model, and thermal plasma in collisional ionization equilibrium, respectively. An index 2 indicates the second spectral component. Luminosities  $L$  are bolometric for an assumed distance of 1 kpc; column densities  $N_{\text{H}}$  are the same for both components, where applicable. References a. Motch et al. 1994 b. Hartmann et al. 1999 c. Ebisawa et al. 2001 d. this paper

instrument	E (keV)	$\Delta E/E$ (1 keV)	model	$T$ ( $10^5$ K)	$g$ ( $\text{cm s}^{-2}$ )	$L$ ( $\text{erg s}^{-1}$ )	$T_2$ ( $10^5$ K)	$L_2$ ( $\text{erg s}^{-1}$ )	$N_{\text{H}}$ ( $\text{cm}^{-2}$ )	$\chi_r^2/\text{dof}$
a ROSAT PSPC	0.1-2.4	0.4	BB	5.6	–	$5 \cdot 10^{38}$			$1.7 \cdot 10^{22}$	1.1/17
b SAX LECS	0.1-10.	0.15	SA	8.75(5)	$10^9$	$4.1 \cdot 10^{36}$			$1.5(2) \cdot 10^{22}$	5.6/15
b SAX LECS	0.1-10.	0.15	SA+TP	8.75(4)	$10^9$	$2.9 \cdot 10^{36}$	80(60)	$< 1.5 \cdot 10^{35}$	$1.4(2) \cdot 10^{22}$	3.4/14
c ASCA SIS	0.4-10.	0.08	BB	5.2	–	$1.8 \cdot 10^{40}$			$2.1 \cdot 10^{22}$	8.1/73
c ASCA SIS	0.4-10.	0.08	SA+TP	10.9	$10^{10}$	$7 \cdot 10^{35}$	12		$1.3 \cdot 10^{22}$	2.0/71
d Chandra HETG	0.4-8.0	0.02	BB	5.2	–	$2.8 \cdot 10^{39}$			$1.6 \cdot 10^{22}$	2.5/252
d Chandra HETG	0.4-8.0	0.02	SA	8.97	$10^9$	$5.3 \cdot 10^{35}$			$1.0 \cdot 10^{22}$	2.9/252
d Chandra HETG	0.4-8.0	0.02	SA+TP	8.96	$10^9$	$4.1 \cdot 10^{35}$	20.6	$4.9 \cdot 10^{34}$	$1.0 \cdot 10^{22}$	2.6/250

## 2. Earlier observations of MR Vel

MR Vel was discovered in the Galactic Plane in the ROSAT All Sky Survey, in a search for supersoft sources. The intrinsic softness of the source combined with strong interstellar absorption cause most of the photons of this source to be detected between 0.5-1.5 keV. A black body fit to the data from a ROSAT PSPC pointing gives a temperature of  $\sim 48$  eV, for an interstellar absorption column of  $\sim 1.7 \cdot 10^{22} \text{ cm}^{-2}$  (Motch et al. 1994). Observations with the BeppoSAX MECS and the ASCA SIS show excess flux at energies  $\gtrsim 1.2$  keV with respect to the flux predicted by black body or stellar atmosphere models. To explain this, a thermal plasma has been suggested as a second component of the spectrum. However, models combining a NLTE white-dwarf atmospheric model with a thermal plasma in collisional ionization equilibrium do not provide acceptable fits to the data, which appear to show absorption edges at 0.87 keV (O VIII), 1.02 keV (unidentified), and 1.36 keV (Ne X), according to Ebisawa et al. (2001).

NLTE atmosphere models give a much lower (unabsorbed) flux for the observations than LTE models, which in turn give lower fluxes than black body fits. Whereas LTE models can give near-Eddington luminosities for MR Vel at a distance of 1 kpc, NLTE models lead to much larger distances or lower luminosities.

Spectral fits to pre-Chandra X-ray data are summarized in Table 1.

A 17<sup>th</sup> magnitude optical counterpart was identified on the basis of a ROSAT HRI position (Motch et al. 1994) and showed a photometric and spectroscopic period of 4.029 d (Schmidtke et al. 2001). The optical lightcurve is asymmetric and single-peaked, with a full amplitude of about 0.3 mag. A shorter, unexplained period of about 0.25 d also appears to be present in the photometry. The very red optical continuum – presumably of the accretion disk – and the very strong interstellar absorption lines indicate a high interstellar absorption, in agreement with

the X-ray results (Motch et al. 1994). Transient satellite lines of the H  $\alpha$  line indicate a transient double-sided jet, with a velocity of  $\sim 5000 \text{ km s}^{-1}$ , and an opening angle between 34 and 80 degrees (Motch 1998). The photometry shows no eclipses, indicating an inclination  $i \lesssim 65^\circ$ .

The radial velocity curve of the He II 4686 and H  $\alpha$  lines, with a semi-amplitude of  $75 \text{ km s}^{-1}$ , with the absence of eclipses lead to a likely donor mass between 1.0 and  $1.6 M_\odot$  for assumed masses between 0.5 and  $1.4 M_\odot$  for the white dwarf. The absence of the donor in the visual spectrum indicates a bright disk, which in turn indicates a minimum distance of a kpc.

## 3. Chandra observations and data analysis

MR Vel was observed on 14/15 November 2000, for a net exposure time of 56.5 ks, using the High-Energy Transmission Grating Spectrometer (HETGS) of the Chandra X-ray Observatory (Canizares et al. 2000 and references therein). The high energy grating (HEG) could not be used for analysis because of a low S/N-ratio. The medium energy grating (MEG) is optimized for the range of 1.2-30  $\text{\AA}$  and provides a spectral resolution of 0.02  $\text{\AA}$  FWHM. The photons are collected at an array of CCDs, ACIS-S, in the focal plane.

The data were processed with standard Chandra X-ray Center software CIAO-2.1, as follows. Photons are extracted by applying a spatial filter around the spectral image, and negatively and positively dispersed spectra are added. Most background photons are recognized by pulse height analysis, and removed; the higher-order spectra of this faint source do not contain useful information. Flux calibration was done with the 1999-07-22 version of the detector response matrix, part of the Chandra calibration database CALDB 2.3.

The errors in each bin with  $N$  photons are approximately Poissonian and given by (see Gehrels 1986):

$$\Delta N = 1 + \sqrt{N + 0.75} \quad (1)$$

ion	number of levels	quantum number	number of transitions
H I	5	5	–
He II	3	3	–
C V	17	4	315
C VI	10	4	285
N VI	17	4	315
N VII	10	4	285
O VI	5	3	153
O VII	17	4	315
O VIII	10	4	285
Ne VII	6	2	2111
Ne VIII	5	3	153
Ne IX	17	4	315
Ne X	10	4	285
Fe XV	19	3	5074
Fe XVI	7	4	184
Fe XVII	21	3	3409
Fe XVIII	2	2	9437
Fe XIX	6	2	23915
Fe XX	8	2	37795
Fe XXI	12	2	34017

**Table 2.** The ions used for the construction of the model atmospheres in TLUSTY, with the respective number of energy levels and the corresponding quantum number up to which all levels are considered. The number of line transitions used by SYNSPEC are also given; these are all transitions between energy levels with quantum numbers from 1 to 10.

For comparison with model spectra, we use  $\chi^2$  fitting and bin the data, until the oversampling of the spectral resolution is less than a factor 3, and until at least 20 counts are present in each energy bin. The resulting spectrum is shown in Fig. 1.

#### 4. Model spectra

We compute NLTE model spectra for white dwarf atmospheres, characterized by effective temperature, gravitational acceleration, and elemental abundances, as described in Hartmann et al. (1999), i.e. using the codes TLUSTY (version 195) for the construction of a model atmosphere, and SYNSPEC (version 42) for the computation of the emergent spectrum. These codes were developed and are described by Hubený (1988) and Hubený & Lanz (1995). For the atmosphere model we use 70 depth zones, and a frequency range from  $10^{12}$  Hz to  $9.6 \cdot 10^{17}$  Hz; convergence is considered to have been achieved when the maximum relative change between subsequent model parameters is less than 0.001. The ions and transitions used in our computations are listed in Table 2; their numbers are limited by computational expense. The atomic data are extracted from the Opacity Project with TOPbase (see Cunto et al. 1993).

Models for thermal plasmas in collisional ionization equilibrium were computed in SPEX, with the code developed and described by Kaastra et al. (1996).

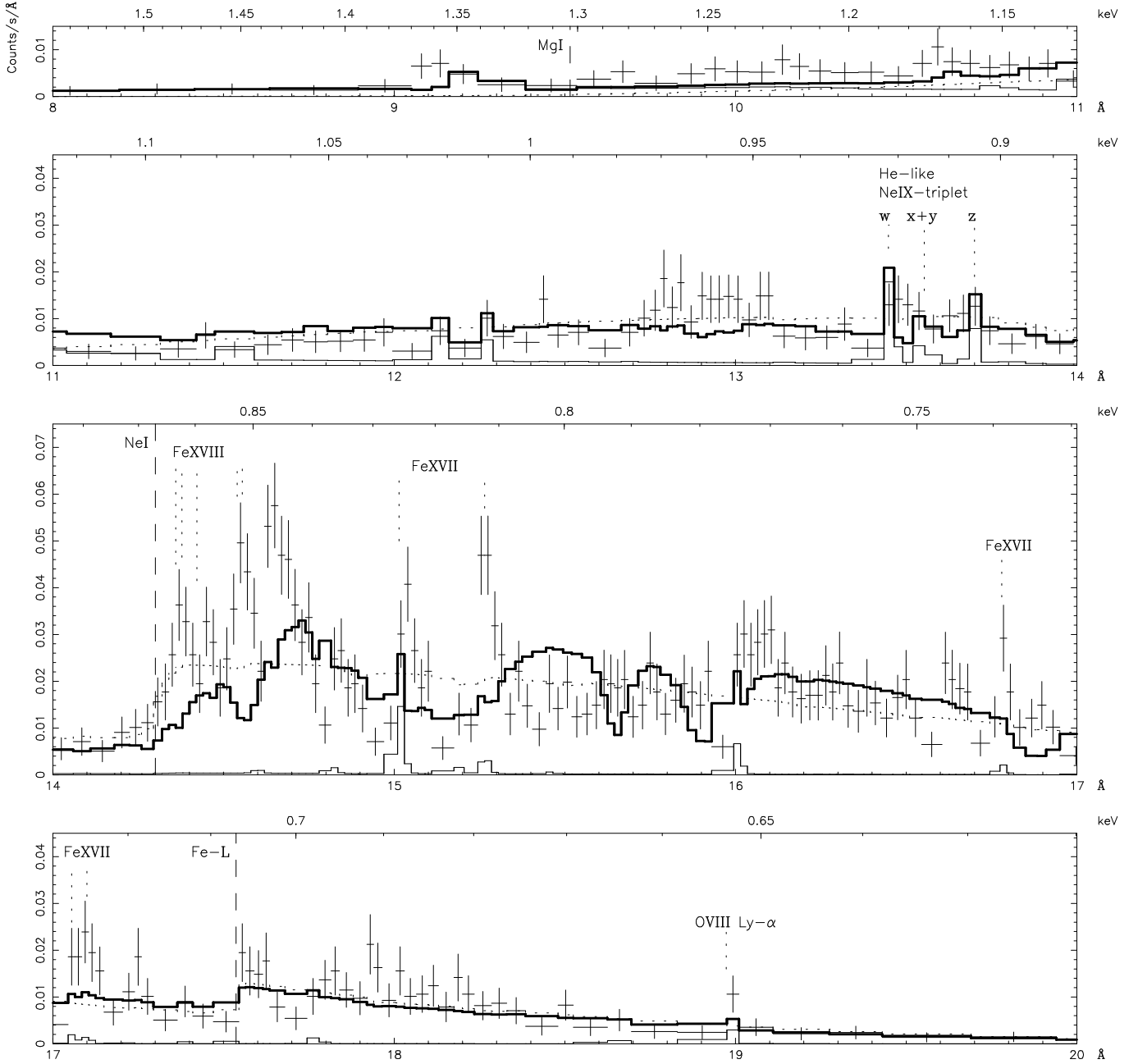


**Fig. 1.** The observed X-ray spectrum of MR Vel binned to the minimum width required for either 1/3 of the instrumental spectral resolution or 20 counts, together with the best black body fit (dotted line) and the best fit combination (thick line) of the spectra from a NLTE atmosphere and a thermal plasma in collisional ionization equilibrium (the latter is also shown separately with a thin line). Some identified spectral features are indicated.

## 5. Results

The observed spectrum shown in Fig.1 shows the following emission lines (with theoretical wavelengths from Phillips et al. 1999). The lines at  $\lambda$  15.014, 15.265, 16.780, 17.055, and 17.100 Å are all due to Fe XVII. The line at  $\lambda$  18.973 Å is the O VIII Lyman  $\alpha$  line. The strong line complex between  $\lambda$  14.3-14.6 Å is a blend of Fe XVIII lines, which cannot be identified individually, the strong feature

at  $\lambda$  14.6-14.7 Å may be a blend of O VIII and Fe XIX lines. The complex of the Ne IX  $\lambda$  13.448, 13.553 and 13.700 Å triplet, respectively the resonance line (w), the intercombination (x+y) lines, and the forbidden (z) line of the He-like ion; these lines are not recognizable individually, but their presence is clear from the enhanced flux in their wavelength range.

We have fitted the observed spectrum with the models discussed by previous authors, i.e. black body, LTE atmo-

sphere and NLTE atmosphere spectra. Following earlier authors, we also added a thermal plasma in collisional ionization equilibrium to a NLTE atmosphere. In Fig. 1 we show the spectra of the best fit black body and the combination of the atmosphere and the plasma. The model parameters are given in Table 1.

The interstellar absorption edges due to Ne I (at  $\lambda 14.30 \text{ \AA}$ ) and Fe-L (at  $\lambda 17.54 \text{ \AA}$ ) are recognizable in the models and in the data, and confirm that interstellar absorption is appreciable. It is clear that neither model is acceptable. The observed spectrum shows much more structure than a black body; but not the structure expected for a calculated atmospheric spectrum. This is true for a gravitational acceleration of  $10^9 \text{ cm s}^{-2}$  and effective temperatures between  $8.00\text{-}9.15 \cdot 10^5 \text{ K}$ .

The combination of a thermal plasma with the NLTE atmosphere indeed adds lines, but the strengths of these are well below those of the observed emission complexes between  $\lambda 14\text{-}16 \text{ \AA}$ . The flux contribution of the plasma is so small that the parameters of the atmospheric model are virtually the same for both models with and without an added thermal plasma. In some calculations we allow an arbitrary global shift in the wavelengths of the lines from the thermal plasma to take into account the current accuracy of the HETG-MEG absolute wavelength calibration; this doesn't change any of the conclusions. Similarly, varying the abundances of iron or oxygen in the thermal plasma only results in marginal improvement; only some emission lines can be reproduced better this way. Assuming different interstellar absorption densities for the two model components, complicates the analysis further with no better results.

If one tries to enhance the emission line strengths by changing the temperature or the emission measure of the plasma, one always finds very strong lines at wavelengths where none are observed. For example, whenever the strength of the Fe XVII lines at  $\lambda 15.014$  and  $15.265 \text{ \AA}$  are enhanced to bring their fluxes to the observed level, the lines from the same ion at  $\lambda 12.124$  and  $12.264 \text{ \AA}$  become too strong. It also produces a thermal continuum which is significantly higher between  $\lambda 7\text{-}12 \text{ \AA}$  than the observed flux.

To compare the relative strengths of the identified Fe XVII lines with theoretical predictions, we have fitted them with Gaussian profiles, as printed in Table 3. No thermal plasma in collisional ionization equilibrium can reproduce the observed relative strengths of the Fe XVII lines, even when we allow a continuous distribution of emission measures as a function of the temperature (the differential emission measure model, see Liedahl et al. 2001). Also the strength of the Fe XVIII lines between  $\lambda 14.3\text{-}14.6 \text{ \AA}$  can't be explained by such plasma. These results remain true when the abundances are varied from solar, because they affect the relative strengths of lines from different elements, not those from the same element.

Theoretical wavelength ( $\text{\AA}$ )	Fitted wavelength ( $\text{\AA}$ )	Relative flux
15.014	$15.05 \pm 0.01$	$0.63_{-0.22}^{+0.25}$
15.265	$15.276 \pm 0.007$	$1.00_{-0.24}^{+0.27}$
16.780	$16.79 \pm 0.01$	$1.61_{-0.78}^{+1.40}$
17.055 / 17.100	$17.10 \pm 0.01$	$3.45_{-1.44}^{+2.20}$

**Table 3.** Parameter values for the fit of the identified Fe XVII lines with gaussian profiles. The two lines at  $\lambda 17.055$  and  $17.100 \text{ \AA}$  are fitted with one profile. The fluxes are printed relative to the flux of the line at  $\lambda 15.265 \text{ \AA}$ , and have been corrected for interstellar absorption with an absorption measure of  $0.99 \cdot 10^{22} \text{ cm}^{-2}$ . Note that this emission feature may have a contribution of the O VIII Lyman  $\gamma$  line.

The main problem is the ratio of the  $15.014 / 15.265$  lines, for which optically thin models predict a value of 3-4 for any density or temperature, while we observe 0.63. The ratio of the  $16.780$  and  $17.055 / 17.100$  lines to the  $15.265$  line is however consistent with an optically thin plasma. Dropping the optically thin assumption, the  $15.014$  line can be brought into agreement with the  $16.780$  and  $17.055 / 17.100$  fluxes for pure Fe XVII column densities of the order of  $10^{19} \text{ cm}^{-2}$ , but also in that case the predicted  $15.014 / 15.265$  ratio still remains similar as in the optically thin case. Thus, also for the optically thick model the  $15.265$  line is 6 times weaker than observed.

We conclude that none of the earlier models describe the observed X-ray spectrum of MR Vel.

We investigate whether the spectrum shows signatures of a photo-ionized plasma, as listed by Liedahl et al. (2001), viz. a) narrow radiative recombination continua; b) large ratio  $(x + y + z)/w$  of the He-like triplet; c) the weakness of L-shell iron emission compared to K-shell emission from lighter elements. The strength of the Fe XVII lines and the relative weakness of the Ne IX lines argues against a photo-ionized plasma. The observed spectrum also does not show evidence for narrow recombination continua. The strengths of the individual Ne lines in the spectrum are too small to determine their ratios. We conclude that a simple photo-ionized plasma also doesn't describe the observations.

## 6. P Cygni profiles indicate a stellar wind

Considering that none of the previously suggested models describes the data, we have another look at the observed spectrum. Fig. 2 gives an expanded view of the five strong, individually identifiable lines and the spectrum around the O VIII Lyman  $\beta$  line at  $16.003 \text{ \AA}$ . The similarity between the profiles of these lines indicates that the P Cygni structure seen in them is real. One would expect to see a similar structure for the Lyman  $\gamma$  and  $\delta$  lines; inspection of the spectra near their wavelengths ( $15.175$  and  $14.817 \text{ \AA}$ , respectively) indeed shows indication of redward

emission and blueward absorption. We conclude from the P Cygni profiles that the stronger individually identifiable lines (see Sect. 5) in our spectrum arise in a wind.

The absorption parts of the O VIII Lyman  $\alpha$  and  $\beta$  and Fe XVII  $\lambda 17.055$  Å lines are saturated; the absorption part of the O VIII Lyman  $\delta$  line is not saturated. For the remaining lines the situation is ambiguous.

Strong P Cygni lines are present in the spectra of high-mass stars, e.g. Wolf-Rayet stars, and also in the spectra of systems with an accretion disk. The radial velocity curve and the absence of strong stellar lines in the optical spectrum, exclude the presence of a high-mass star in MR Vel (see Sect. 2). Thus, the P Cygni profiles in the X-ray spectrum of MR Vel are more likely related to the presence of an accretion disk.

In cataclysmic variables, the terminal wind velocities are often fairly high, reaching values of  $5000 \text{ km s}^{-1}$  (e.g. Woods et al. 1992). The similar velocity of the transient jet seen in the optical has been used by Motch (1998) to argue that the accreting object is a white dwarf. Remarkably, the highest absorption velocities seen in Fig. 2 are rather lower, of the order of  $1500 \text{ km s}^{-1}$ .

It seems possible that a combination of an atmosphere spectrum with P Cygni profiles from a wind gives a good description of the X-ray spectrum of MR Vel. It is beyond the scope of this article to construct such a model. At this point we repeat our earlier statement that no obvious atmospheric features can be seen in the X-ray spectrum, as shown in Fig. 1.

## 7. Discussion

The observed X-ray spectrum of MR Vel is dominated by emission features, and is not the continuum with absorption features expected on the basis of stellar atmosphere models, nor is it an optically thin spectrum of a thermal plasma in collisional ionization equilibrium, or a photoionized plasma. Instead, we suggest that the spectrum is a combination of a stellar atmosphere and a wind.

The bulk of the luminosity of the models fitted by earlier authors lies outside the observed X-ray regimes, at softer energies. As a result the luminosities derived from the same observations range from above the Eddington limit for a black body to less than 0.001 of the Eddington limit for the spectrum of a NLTE atmosphere, as can be observed in Table 1. The uncertain magnitude of the interstellar absorption adds to the uncertainty. This also may be seen in Table 1, by comparing the same model fitted to data of different satellites.

Therefore we cannot predict the bolometric luminosity corresponding to the X-ray spectrum of MR Vel. This remains true for models with a wind. We can only determine the luminosity in the observed range of  $8\text{-}20$  Å at  $\sim 10^{35} \text{ erg s}^{-1}$  for an assumed distance of 1 kpc. As a result, we can no longer be certain that MR Vel is as

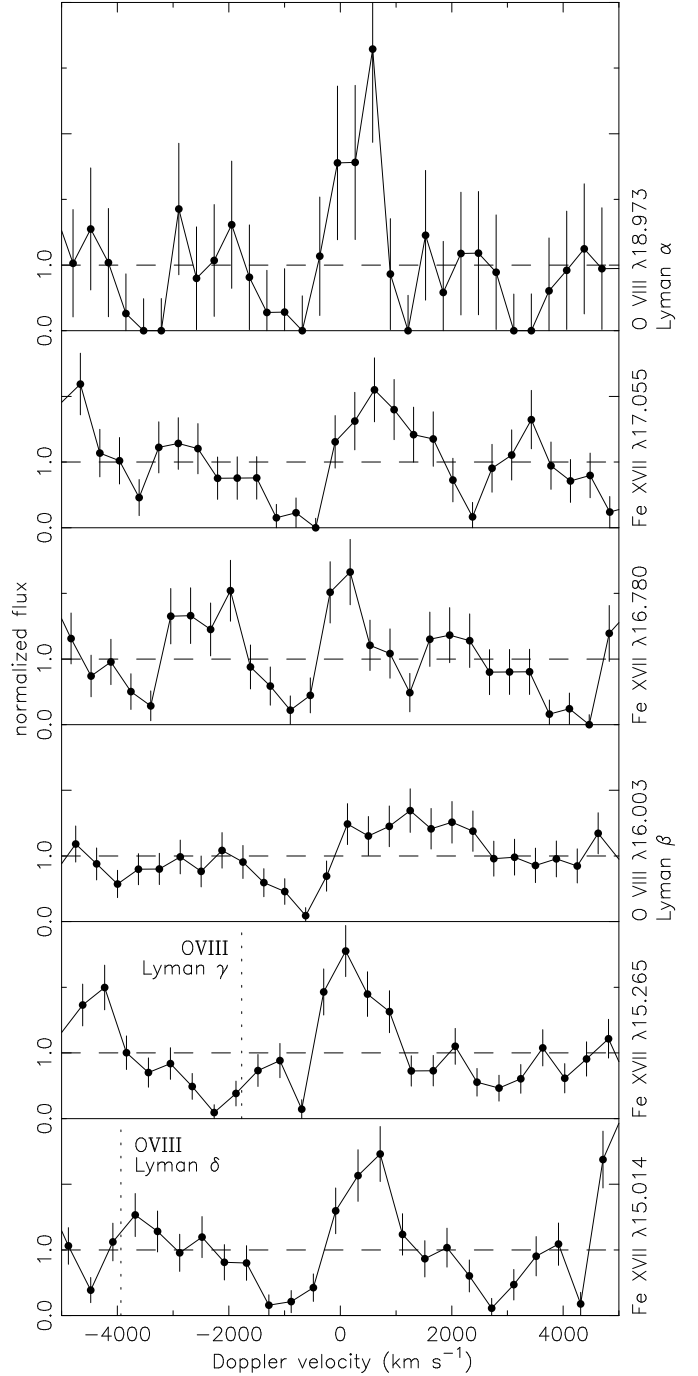


**Fig. 2.** Profiles of some strong, individually identifiable lines in the spectrum of MR Vel. The average flux in each frame has been normalized to unity; this level is indicated with the dashed lines. The wavelength scale is given in Doppler velocities, based on central wavelengths shown on the right of each frame; the wavelength resolution is the instrumental resolution, i.e. more points are shown than in Fig. 1. The central wavelengths of the oxygen Lyman  $\gamma$  and  $\delta$  lines are indicated with vertically dotted lines in the two lower frames.

luminous as expected for a white dwarf steadily burning helium at its surface.

One of the other supersoft sources, Cal 83, has been observed with the reflection grating spectrograph of XMM, with a resolution of 0.05 Å in the range of interest for this softer source, 20-38 Å (Paerels et al. 2001). At first glance, the observed spectrum of Cal 83 could consist of either emission features with a width of  $\sim 1$  Å, or a continuum with many absorption features of comparable width. Paerels et al. prefer the latter interpretation, but cannot match the absorption features with features from an atmosphere dominated by CNO, or from a model with element abundances as appropriate for the LMC, up to Fe. At the moment then, the bolometric flux of Cal 83 also is unknown.

Before definite conclusions can be drawn about the nature of the supersoft sources, more progress is required in the theoretical description of their X-ray spectra. In particular, it seems necessary to develop models that combine atmosphere models with winds. The atmosphere models themselves can be improved with respect to the current models in several ways. More elements and ions can be included in the computation of the atmospheric structure, with a more complete account of the line-blanketing effects. Gradients in temperature and gravitational acceleration, as can be expected for accretion disk spectra, cannot be ruled out. Non-static or outflowing atmospheres may have to be considered. The question arises whether the jet observed in MR Vel and the winds observed in several supersoft sources contribute to their X-ray spectra.

#### *Acknowledgements*

We thank Herman Marshall at the Chandra Science Center for his support in this observation.

The Laboratory for Space Research Utrecht is supported financially by NWO, the Netherlands Organization for Scientific Research.

#### **References**

- Canizares, C., Huehmoerder, D., Davis, D. et al., 2000, ApJ 539, L41
- Cash, W., 1979, ApJ 228, 939
- Cunto, W., Mendoza, C., Ohsenbein, F., & Zeppen, C.J., 1993, A&A 275, L5
- Dotani, T., Asai, K., & Greiner, J., 1999, Publ. Astr. Soc. Japan 51, 519
- Ebisawa, K., Mukai, K., Kotani, T. et al., 2001, ApJ 550, 1007
- Gänsicke, B., van Teeseling, A., Beuermann, K., & Reinsch, K., 2000, New Astronomy Review 44, 143
- Gehrels, N., 1986, ApJ 303, 336
- Greiner, J., Hasinger, G., & Kahabka, P., 1991, A&A 246, L17
- Hartmann, H. & Heise, J., 1997, A&A 322, 591
- Hartmann, H., Heise, J., Kahabka, P. et al., 1999, A&A 346, 125
- Heise, J., van Teeseling, A., & Kahabka, P., 1994, A&A 288, L45
- van den Heuvel, E., Bhattacharya, D., Nomoto, K., & Rappaport, S., 1992, A&A 262, 97
- Hubený, I., 1988, Computer Physics Comm. 52, 103
- Hubený, I. & Lanz, T., 1995, ApJ 439, 875
- Iben, I., 1982, ApJ 259, 244
- Kaastra, J., Mewe, R., & Nieuwenhuijzen, H., 1996, in K. Yamashita and T. Watanabe (eds.), UV and X-ray spectroscopy of astrophysical and laboratory plasmas, p. 411, Univ. Acad. Press
- Liedahl, D.A., Wojdowski, P.A., Jimenez-Garate, P.S.W.M.A. & Sako, M., 2001, to appear in the proceedings of The Challenge of High Resolution X-ray through Infrared Spectroscopy, p. 5084, Lexington
- Long, K., Helfand, D., & Grabelsky, D., 1981, ApJ 248, 925
- Mewe, R., Kaastra, J., & Liedahl, D., 1995, Legacy 6, 16
- Motch, C., 1994, A&A 338, L13
- Motch, C., Hasinger, G., & Pietsch, W., 1994, A&A 284, 827
- Ögelman, H., Orio, M., Krautter, J., & Starrfield, S., 1993, Nat 361, 331
- Paerels, F., Rasmussen, A.P., Hartmann, H.W. et al., 2001, A&A 365, L308
- Phillips, K.J.H., Mewe, R., Harra-Murnion, L.K et al., 1999, A&A 138, 381
- Schmidtke, P.C., & Cowley, A.P., 2001, ApJ 122, 1569
- Shara, M.M., Prialnik, D., & Shaviv, G., 1977, A&A 61, 363
- Trümper, J., Hasinger, G., Aschenbach, B. et al., 1991, Nat 349, 579
- Wood, J. & Lockley, J., 2000, MNRAS 313, 789
- Woods, J.A., Verbunt, F., Collier Cameron, A. et al., 1992, MNRAS 255 237